

Multi-wavelength polarization VLBI observations of two BL Lac objects

Vladislavs Bezrukovs¹

Cork Institute of Technology, Ireland

E-mail: s_bezrukovs@inbox.lv

Denise Gabuzda

University College Cork, Ireland

E-mail: gabuzda@phys.ucc.ie

We present results of intensity and linear polarization imaging and model fitting for two sources based on VLBA observations for a sample of 1-Jy northern BL Lac objects. Observations were carried out in August 2004 at 43, 22 and 15 GHz. The observed polarization vectors in the jets are aligned with the jet, implying the presence of transverse magnetic fields. We confirm the presence of a transverse Faraday rotation gradient across the jet of 1803+784, providing evidence that this jet has a helical magnetic field.

*The 8th European VLBI Network Symposium
September 26-29, 2006
Toruń, Poland*

¹ Speaker

1. Introduction

BL Lacertae (BL Lac) objects are active galactic nuclei displaying weak, sometimes undetectable, optical line emission and strong variability in total intensity and linear polarization from the optical through the radio domain. They have compact radio structure with flat or inverted radio spectra. For some, luminous elliptical host galaxies are observed (Angel & Stockman 1980; Miller 1981). The radio emission and much of the optical emission is believed to be synchrotron radiation.

Previous VLBI polarization observations of radio-bright BL Lac objects have shown certain characteristic properties on parsec scales: one-sided core-jet structures having superluminal motions with typical speeds, on average, lower than those in quasars; polarization vectors parallel to the local jet axis, and a tendency for the core polarization vectors to lie either parallel or perpendicular to the jet axis (Gabuzda, Pushkarev & Cawthorne 2000). The tendency for the optically thin jet polarization vectors to align with the jet direction implies that the associated magnetic B fields are predominantly transverse. Most recently, such transverse fields have been taken to reflect the presence of helical B fields associated with the jets (Gabuzda 1999; Gabuzda et al 2004; Pushkarev et al 2005; Lyutikov et al 2005, Gabuzda 2007).

The observations of the sources for which results are presented here were made as a part of a programme to obtain 43, 22 and 15-GHz total intensity and polarization VLBI images for all sources in the Kühr & Schmidt (1990) complete sample of 34 radio-bright BL Lac objects in the northern sky.

2. Observation

Observations of 7 BL Lac objects in the Kühr & Schmidt (1990) sample were made on 24 Aug 2002 using the VLBA. The observations were carried out at 43, 22 and 15 GHz with full polarization information. The data were correlated using the VLBA correlator in Socorro, New Mexico.

The data were calibrated and imaged with the NRAO AIPS package using standard techniques. We determined the instrumental polarizations (D-terms) of each antenna for each frequency using AIPS task LPCAL, solving simultaneously for the polarizations of individual regions in the compact calibrators used. The absolute orientation of the polarization angles was calibrated by comparing the integrated polarization angles with the polarization angles for the total VLBA-scale polarization for several compact sources. The VLBA and integrated polarization measurements were not strictly simultaneous, but the good consistency in the results obtained for different sources leads us to believe that the resulting polarization angles, χ , are accurate to within about 5° .

3. Results

Results for two sources are discussed below. The total intensity maps with polarization vectors superimposed are shown in Figs 1 and 4. In each of the images, the restoring beams are shown as an ellipse in a corner of the images.

Preliminary models of the source structures were derived by fitting the complex total intensity (**I**) and polarization (**P**) visibilities that come from the hybrid mapping process. **I** was fitted with circular Gaussian components and **P** was fitted with delta function components using the programme VISFIT (Roberts et al. 1987, Gabuzda, Wardle & Roberts 1989a). The **I** components are shown in the images as dark green circles, whose size corresponds to the size of the Gaussian component. The **P** components are shown as dark blue sticks, whose angle corresponds to the polarization angle. In all cases, consistency between the model-fitting results, the distribution of the CLEAN components, and the visual appearance of the images was checked. Components were included in the models only if there was clear evidence for them in the CLEAN components derived during the image process. The **I** and **P** visibilities were fitted separately in order to allow for small differences in the positions of corresponding **I** and **P** components, either intrinsic to the source structure or resulting from residual calibration errors.

VISFIT, an **I** and **P** model fitting programme running under Linux, has now been tested. Anyone wishing to obtain more information about this software or to receive a copy should feel free to contact the authors.

3.1 1308+326

The classification of the high redshift ($z = 0.997$) source 1308+326 is uncertain. It has been labelled a BL Lac because of its almost featureless optical spectrum, strong optical variability and the high degree of polarization of its optical continuum; however, 1308+326 also exhibits quasar-like properties (see the discussion in Gabuzda et al 1993).

In our images (Fig. 1), the jet extends toward the north-west and, at a distance of 1.5 mas, changes its direction to the west. In the outer jet, polarization vectors are aligned with the jet direction; this is not clear in the 15-GHz map, but in 22-GHz image, the polarization component in the jet (dark blue stick in Fig. 1.b) coincides with the jet in this region very clearly. Thus, the outer jet magnetic field is predominantly transverse. In contrast, the **B** field in the inner jet seems to be longitudinal.

The positions of the **I** and **P** model fit components for the three frequencies are in a good agreement. Although, in some cases, there are small offsets between the corresponding components at different frequencies (within the errors), there are no systematic offsets with frequency, as would be expected for significant frequency dependence for the core position (Lobanov 1996). At 43 GHz, an additional **I** component located close to the core has been found.

The spectral index maps show that, between 22 GHz and 43 GHz, the core changes from optically thick (Fig. 2.a) to optically thin (Fig. 2.b). This is also visible as a roughly 90° rotation in polarization angle for the core between 22 and 43 GHz. Accordingly, before determining the core Faraday rotation measure, we rotated the polarization position angle by 90° at 43 GHz.

Fig. 3. shows the χ_{core} values as a function of the wavelength squared. The black line rotation measure (RM) was calculated from the original χ values (black circles). The red square represents χ_{core} shifted by 90° at 43 GHz, and the red line corresponds to the resulting RM value. This gives us a good RM linear fit. We thus calculated the core rotation measure to

be $\sim +3220 \text{ rad}/m^2$. This is substantially higher than the core RM found for 15-GHz + 8.4-GHz VLBA polarization data, $\sim +115 \text{ rad}/m^2$ (Zavala & Taylor 2003). The most likely reason for this is a higher free electron density on the smaller scales probed by our higher frequency observations.

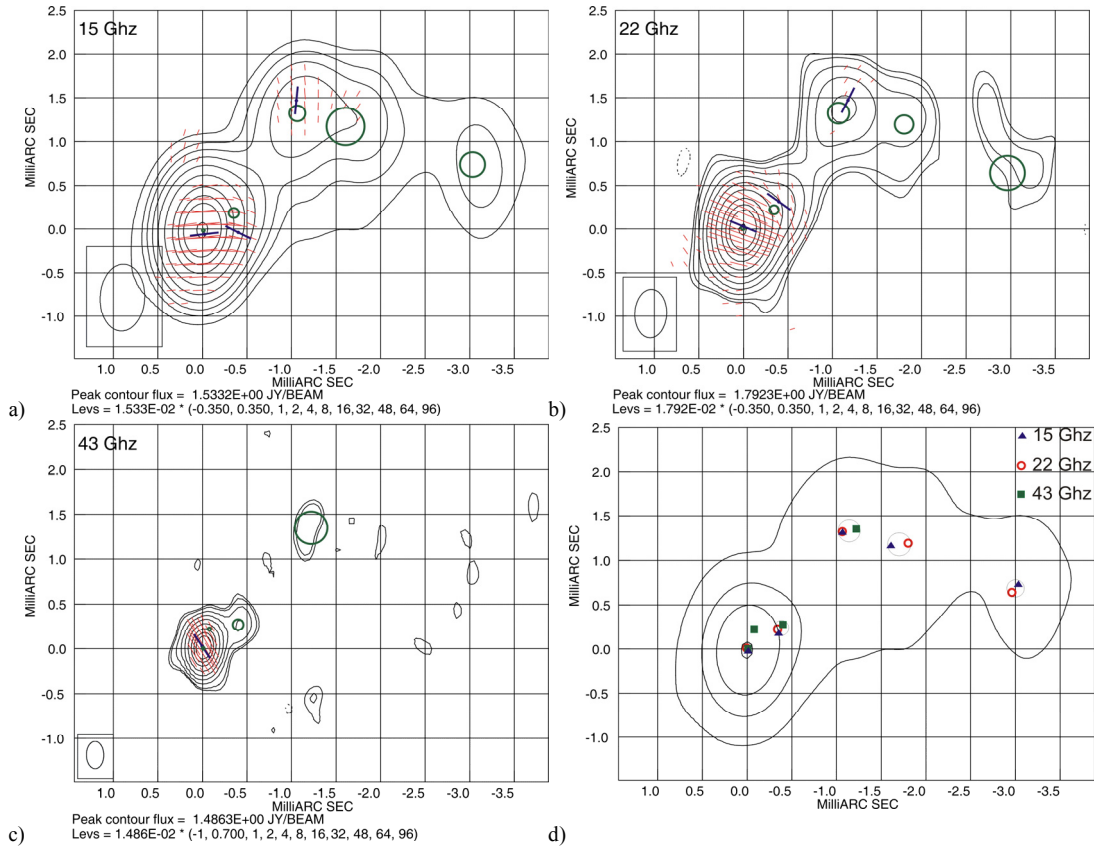


Figure 1. Total intensity (contours) and polarization (red sticks) maps of source 1308+326 with intensity (dark green circles) and polarization (dark blue sticks) model fitting components. a) at 15 GHz; b) at 22 GHz; c) at 43 GHz; d) Intensity contours at 15 GHz and intensity model fitting components.

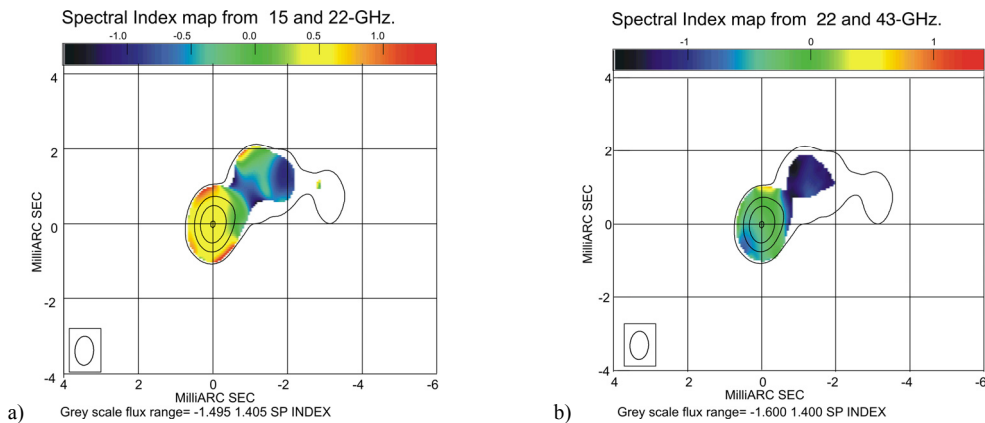


Figure 2. Spectral index maps of source 1308+326 for a) 15 and 22 GHz; b) 22 and 43 GHz.

POS(8LHEVN)027

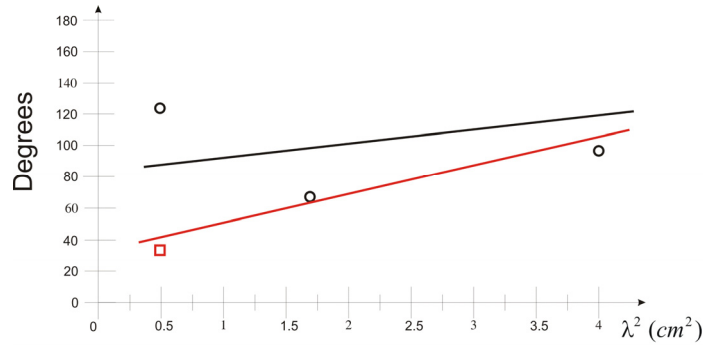


Figure 3. Rotation measure for source 1308+326 core. Black line – original polarization angles; Red line – rotation measure with polarization angle at 43 GHz rotated by 90°.

3.2 1803–784

1803-784 has a redshift $z = 0.68$. The dominant orientation of the inner ~ 10 mas of the VLBI jet is nearly exactly westerly (Witzel et al. 1988; Gabuzda et al 1992); further from the core, the jet begins to curve to the south (Britzen et al 1999), toward the arcsec-scale structure (Kollgaard et al 1992). Evidence for motion on smaller scales that is not collinear with the dominant east-west structure has been found in VLBI studies at higher frequencies (e.g. Krichbaum et al 1993) or with polarization (Gabuzda 1999).

The positions of the intensity model fit components coincide at all frequencies (Fig. 4). As for 1308+326, we find no evidence for a significant frequency-dependent core shift. We found two polarization components at all frequencies, whose positions and polarizations agree. The polarization vectors are aligned with the jet direction, indicating a magnetic field transverse to jet.

We calculated a rotation measure map based on the 43, 22 and 15-GHz data (Fig. 5.a). The RM of the core is about $+500 \text{ rad}/m^2$, somewhat larger than the VLBI core rotation measures reported previously for this source based on the VLBA data at lower frequencies, $\sim -200 \text{ rad}/m^2$ (Gabuzda, Chernetskii 2003; Zavala, Taylor 2003). In addition, we find a positive core RM, while observations at lower frequencies have found a negative RM. This may indicate changes in the orientation of the line-of-sight component of the B field, as discussed by O’Sullivan & Gabuzda (2007). We found an asymmetric RM distribution across the jet. The RM changes from $\sim 2000 \text{ rad}/m^2$ on the north side, to almost $\sim 0 \text{ rad}/m^2$ on the south side. This RM gradient in jet can be very naturally interpreted in terms of a helical magnetic field, as described by Asada et al (2002) and Gabuzda et al (2004). An RM gradient across the jet of this source with the same orientation as in our data was also found at lower frequencies by Mahmud and Gabuzda (2007) the RM map of Zavala and Taylor (2003) also shows a transverse gradient, but in the opposite direction: RM decreasing from south to north (Fig. 5.b). It may be that this indicates some mechanism that can change the helicity of the jet B field with time (see also Mahmud & Gabuzda 2008).

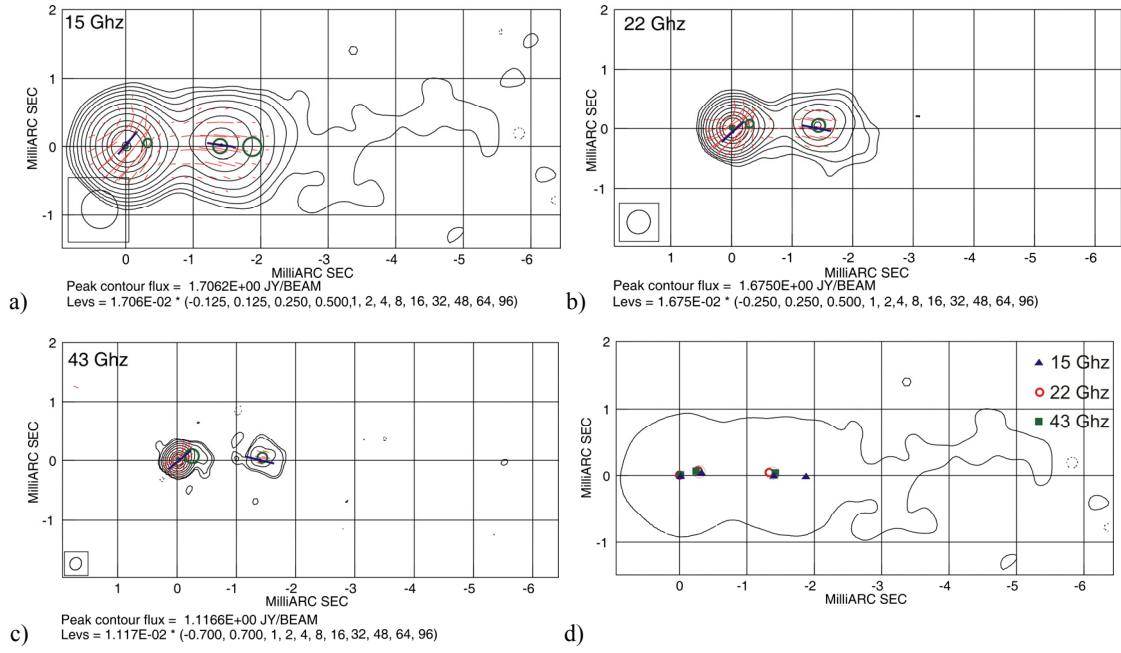


Figure 4. Total intensity (contours) and polarization (red sticks) maps of source 1803+784 with intensity (dark green circles) and polarization (dark blue sticks) model fitting components. a) at 15 GHz; b) at 22 GHz; c) at 43 GHz; d) Intensity contours at 15 GHz and intensity model fitting components.

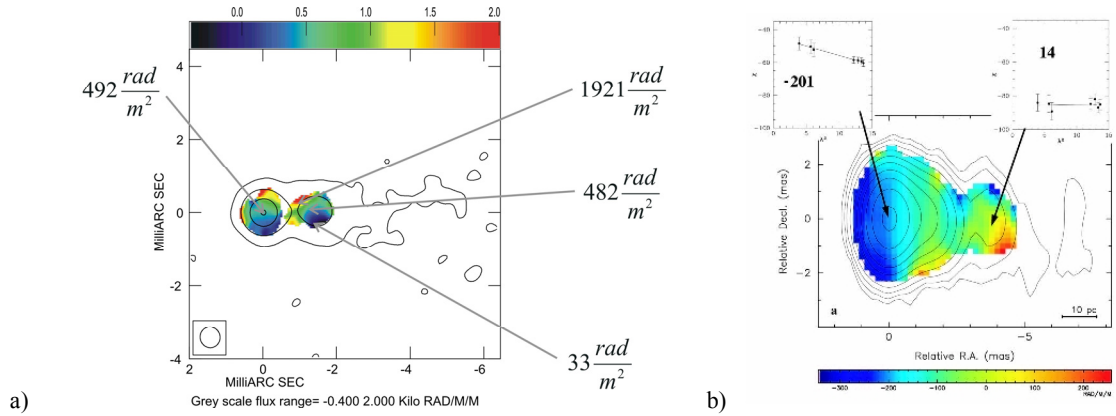


Figure 5. Rotation measure map of source 1803+784 a) from 15, 22, 43 GHz which show asymmetric RM distribution across the jet and b) Zavala and Tailor 2003 RM map with gradient in jet.

4. Acknowledgments

Vladislavs Bezrukovs would like to thank the European Marie Curie Actions under Research and Travel grant and ENIGMA Irish group for their support.

References

[1] Asada, H; Inoue, M; Uchida, Y; Kameno, S; Fujisawa, K; Iguchi, S; Mutoh, M, 2002. Publications of the Astronomical Society of Japan, Vol.54, No.3, pp. L39-L43

[2] Angel, J. R. P.; Stockman, H. S. Optical 1980. Annual review of astronomy and astrophysics. Vol. 18, p. 321-361.

- [3] Britzen, S.; Witzel, A.; Krichbaum, T. P.; Muxlow, T. W. B. 1999. *New Astronomy Reviews*, Vol. 43, Issue 8-10, p. 751-755.
- [4] Gabuzda, D. C.; Murray É.; Cronin P., 2004. *Monthly Notices of the Royal Astronomical Society*, Volume 351, Issue 9, pp. L89-L93.
- [5] Gabuzda D. C. and V. A. Chernetskii, 2003. *Monthly Notices of the Royal Astronomical Society*, 339, 669.
- [6] Gabuzda, D. C.; Pushkarev, A. B.; Cawthorne, 2000. T. V. *Monthly Notices of the Royal Astronomical Society*, Volume 319, Issue 4, pp. 1109-1124.
- [7] Gabuzda D. C., 1999. *New Astronomy Reviews*, 43, 691 (1999).
- [8] Gabuzda, D.C., 2007, 8th EVN Symposium, 2006, ed. A. Marecki, [PoS\(8thEVN\)011](#).
- [9] Gabuzda D. C., J. F. C. Wardle, and D. H. Roberts, 1989. *Astrophysical Journal*, 338, 743.
- [10] Kollgaard, R. I.; Wardle, J. F. C.; Roberts, D. H.; Gabuzda, D. C. 1992. *Astronomical Journal*, vol. 104, no. 5, p. 1687-1705.
- [11] Krichbaum, T. P.; Witzel, A.; Graham, D. A.; Schalinski, C. J.; Zensus, J. A. 1993. *Proceedings of the Nuffield Radio Astronomy Laboratories' conference*, held in Manchester, July 20-24, 1992. p.181
- [12] Kühr, H.; Schmidt, Gary D. 1990. *Astronomical Journal*, vol. 99, Jan. 1990, p. 1-6.
- [13] Lyutikov, M.; Pariev, V. I.; Gabuzda, D. C. 2005. *Monthly Notices of the Royal Astronomical Society*, Volume 360, Issue 3, pp. 869-891.
- [14] Lobanov A. 1996. PhD thesis, New Mexico Institute of Mining & Technology, Socorro, NM, USA.
- [15] Mahmud, M., Gabuzda, D.C., 2007, 8th EVN Symposium, 2006, ed. A. Marecki, [PoS\(8thEVN\)012](#).
- [16] Mahmud, M., Gabuzda, D.C., 2008. *Proceeding of the conference "Extragalactic Jets: Observations and Theory from Radio to Gamma-rays"*, in press.
- [17] Miller, J. S. 1981. *Astronomical Society of the Pacific, Publications*, vol. 93, Dec. 1981, p. 681-694.
- [18] O'Sullivan, S., Gabuzda, D.C., 2007, 8th EVN Symposium, 2006, ed. A. Marecki, [PoS\(8thEVN\)014](#).
- [19] Pushkarev, A. B.; Gabuzda, D. C.; Vetukhnovskaya, Yu. N.; Yakimov, V. E. 2005. *Monthly Notices of the Royal Astronomical Society*, Volume 356, Issue 3, pp. 859-871.
- [20] Roberts, David H.; Gabuzda, Denise C.; Wardle, John F. C. 1987. *Astrophysical Journal*, Part 1, vol. 323, Dec. 15, 1987, p. 536-542.
- [21] Zavala, R.T.; Taylor, G.B. 2003. *The Astrophysical Journal*, Volume 589, Issue 1, pp. 126-146.